atmosphere

MDPI

Article

Moisture Variability in the East Pearl River Basin since 1894 CE Inferred from Tree Ring Records

Teng Li [1,*], Jinbao Li [2,3], Tsun Fung Au [4] and David D. Zhang [1]

1 School of Geography and Remote Sensing, Guangzhou University, Guangzhou 510006, China; dzhang@gzhu.edu.cn
2 Department of Geography, University of Hong Kong, Hong Kong SAR 999077, China; jinbao@hku.hk
3 HKU Shenzhen Institute of Research and Innovation, Shenzhen 518057, China
4 Department of Geography, Indiana University, Bloomington, IN 47405, USA; tomau123@indiana.edu
* Correspondence: liteng@gzhu.edu.cn

Received: 19 September 2020; Accepted: 6 October 2020; Published: 9 October 2020

Abstract: Short-term climate change in South China has been extensively studied based on meteorological or hydrological records. However, tree ring-based long-term climate change research is rare, especially in the Pearl River basin, owing to the difficulty in finding old-aged trees. Here, we present a 200-year tree ring width chronology of *Pinus kwangtungensis* in the east Pearl River basin with reliable coverage from 1894 to 2014. Based on the significant climate-growth relationship between tree growth and annual self-calibrating Palmer drought severity index (scPDSI) from previous May to current April, the pMay-cApr scPDSI was reconstructed for the period 1894–2014. The reconstruction reveals four dry periods during 1899–1924, 1962–1974, 1988–1994, and 2003–2014, and four wet periods during 1894–1898, 1925–1961, 1975–1987, and 1995–2002. Significant spatial correlations between the reconstructed scPDSI and the Climatic Research Unit (CRU) gridded scPDSI indicate that our reconstruction can effectively represent regional moisture variability in the Pearl River basin. Spatial correlations with global sea surface temperatures (SSTs) show that our reconstruction is negatively correlated with northern and western Pacific SSTs while positively correlated with eastern Pacific SSTs, suggesting that SST variability in these domains strongly affects moisture change in the Pearl River basin.

Keywords: moisture; tree ring; climate change; PDSI; Pearl River basin

1. Introduction

Short-term climate change in the Pearl River basin has been effectively elucidated based on instrumental records. For instance, under the background of global warming, temperature in the Pearl River basin increased over 1956–2013, with a greater warming rate in winter than in summer [1]. As for moisture conditions, the Pearl River basin showed a tendency to be drier during 1960–2005 [2]. Zhang et al. [3] indicated that increasing temperature significantly contributes to the drying tendency, especially in autumn and winter. Nonetheless, the short instrumental records limit the understanding of climate change in the Pearl River basin from a long-term perspective.

Owing to the advantages of annual resolution, accurate dating, and high sensitivity to climate, tree ring records provide reliable long-term information on past climate variations [4]. As one of the paleoclimatic proxies, tree ring records have been successfully applied to reconstruct past climate change worldwide and to evaluate decadal or multi-decadal climate variations [5–16]. However, due to the lack of old-aged trees and the complex relationship between tree growth and climate in subtropical China, very few tree ring studies have been conducted in South China, and those available are mostly conducted in Southeast and Southwest China [17–24]. Even fewer tree ring studies have

been conducted in the Pearl River basin. *Pinus kwangtungensis* is an endemic species in South China and grows mostly in south Hunan, south Guizhou, southwest Guangxi, and north Guangdong at altitudes of 700–1600 m a.s.l. [25]. To our knowledge, no dendroclimatic studies have been conducted on *P. kwangtungensis* in the Pearl River basin yet. Therefore, this study aims to fill this research gap by developing the tree ring width (TRW) chronology of *P. kwangtungensis* in the east Pearl River basin. Specifically, the objectives of this study are to (1) develop a TRW chronology of *P. kwangtungensis* from a sampling site in the east Pearl River basin; (2) reconstruct past moisture variability using the TRW chronology; and (3) investigate the linkages between regional moisture variations and the Pacific and Indian Ocean sea surface temperatures (SSTs).

2. Materials and Methods

2.1. Tree Ring Data

Tree cores of *P. kwangtungensis* were taken from Mount Xiaohuangshan (XHS) in the northern Guangdong Province of South China, at an elevation of around 1403 m a.s.l. (Figures 1 and 2). Two cores were taken from each tree with 5.1-mm-diameter increment borers. After air drying, mounting, and sanding, all tree cores were visually cross-dated under microscope and measured on a Velmex ring width measuring system with a resolution of 0.001 mm. The quality and accuracy of cross-dating and measurement were checked using the program COFECHA [26]. Finally, 35 cores from 20 trees were used to build the mean ring width chronology (Table 1). All the series were standardized to remove the non-climatic growth signals contained in the raw ring width measurements [4,26]. Logarithmic transformation was applied to stabilize the variance in order to meet the requirement of normality. The tree ring indices were calculated as residuals between raw ring width series and a fitted age-dependent growth curve, and the extreme values of the tree ring indices were reduced by a biweight robust mean method [27,28]. After detrending, the Rbar weighted method was applied for variance stabilization of the chronology [29,30]. The "signal-free" method was used to minimize the "trend distortion" problem [31]. Rbar and Expressed Population Signal (EPS) with a threshold value of 0.85 were employed to assess the stability and reliability of the chronology over time [32].

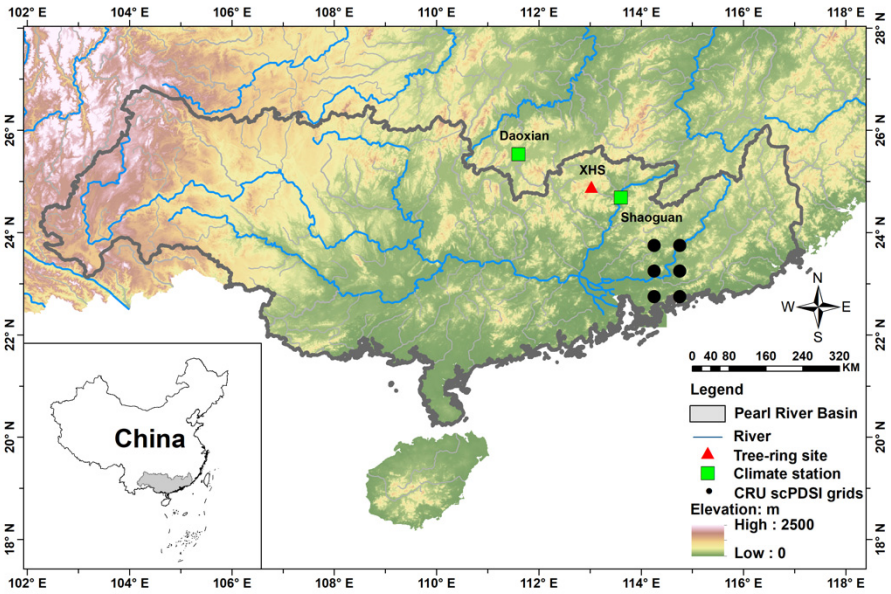

Figure 1. Map of the Pearl River basin showing the location of the tree ring sampling site (red triangle), nearby meteorological stations (green square), and the Climatic Research Unit (CRU) self-calibrating Palmer drought severity index (scPDSI) grids (black circle).

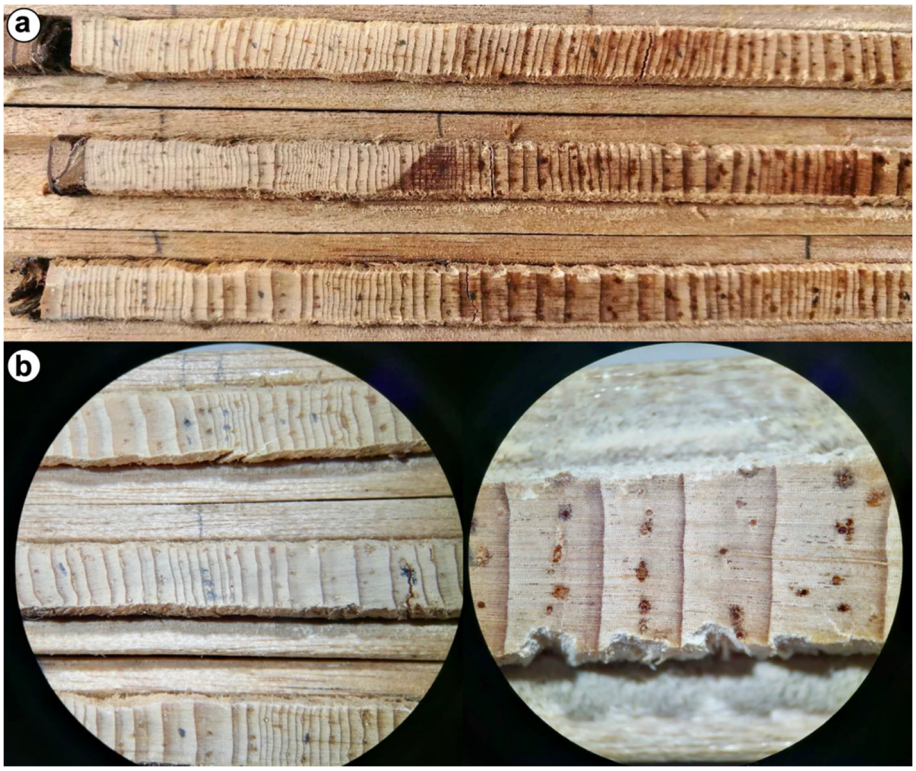

Figure 2. (**a**) Image of *Pinus kwangtungensis* tree core samples and (**b**) high-resolution image of annual growth layers of *Pinus kwangtungensis* under microscope.

Table 1. Site information and tree ring chronology statistics.

Site Code	Location (Latitude, Longitude)	Elevation (m a.s.l.)	Cores/Trees	Time Span (AD)	SD	MS	AC1	Rbar	EPS
XHS	24.90° N, 113.02° E	1403	35/20	1815–2014	0.21	0.29	0.65	0.26	0.92

SD, standard deviation; MS, mean sensitivity; AC1, first-order autocorrelation; Rbar, within trees rbar; EPS, expressed population signal.

2.2. Climate Data

Monthly temperature and precipitation records of two nearby meteorological stations (Daoxian, 25.53° N, 111.60° E, 192.2 m a.s.l., 1960–2016, and Shaoguan, 24.68° N, 113.60° E, 61.0 m a.s.l., 1951–2016, Figure 1) were obtained from the National Meteorological Information Centre of China (http://data.cma.cn/). According to the instrumental records, the annual mean temperature of Daoxian (Shaoguan) is about 18.7 °C (20.4 °C), with the highest temperature in July of 28.9 °C (29.0 °C) and the lowest temperature in January of 7.3 °C (10.1 °C), respectively (Figure 3). The annual total precipitation of Daoxian (Shaoguan) is approximately 1336.9 mm (1570.7 mm), with March–August precipitation accounting for 72.0% (74.0%) of the annual total precipitation.

Based on the temperature and precipitation data, as well as a soil moisture supply and demand model, the Palmer drought severity index (PDSI) was designed to quantify the soil moisture balance over a location [33]. To make the results from different regions more comparable, the self-calibrating PDSI (scPDSI) was introduced by dynamically calculating the climatic factors with fixed parameters based on the actual soil/surface characteristics of a given location [34]. Compiled by the Climatic Research Unit (CRU) at the University of East Anglia (http://www.cru.uea.ac.uk/) [35], monthly scPDSI grids over the Pearl River basin were used to detect the tree growth response to soil moisture balance (Figure 1).

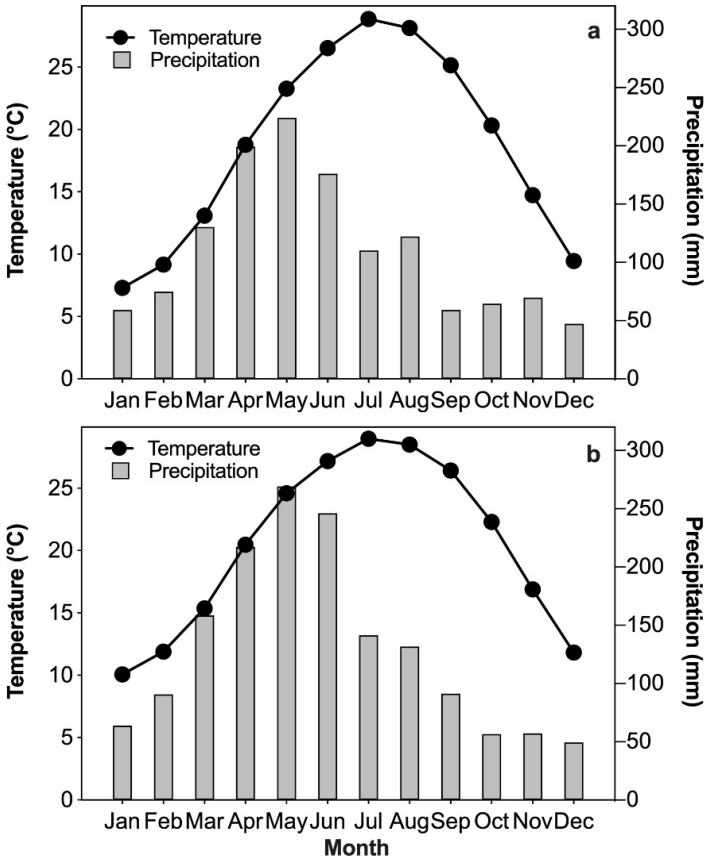

Figure 3. Monthly mean temperature (line with symbols) and monthly total precipitation (bar) from (**a**) Daoxian (1960–2016) and (**b**) Shaoguan (1951–2016) meteorological stations.

2.3. Statistical Methods

Pearson's correlation analysis was applied to reveal the relationship between tree growth and climate factors from the previous March to current October. In addition to monthly correlations, correlations on multiple monthly scales were also calculated because tree growth may be more responsive to quasi-seasonal climate variables [6]. As for CRU scPDSI grid data, the average of various combinations of grid points over the east Pearl River basin and near the tree ring site were used to correlate with the TRW chronology during the common period of the instrumental records. The grid points with the highest correlations were selected for reconstruction (Figure 1). A linear regression model between the TRW chronology and the targeted climatic parameter was used to build the reconstruction [4,27]. The reconstruction was performed with principal components Regression Program (PcReg, available at https://www.ldeo.columbia.edu/tree-ring-laboratory/resources/software). The split-sample calibration verification and leave-one-out cross-validation (LOOCV) method were applied to test the quality and stability of the regression model [36]. Reduction of error (RE) and coefficient of efficiency (CE) were used to assess the skill of the regression model. RE and CE values that exceed zero indicate good model skill [4]. To evaluate the influence of trend on the reconstruction model, the first-differenced reconstructed and observed data were compared during their common period. We have also identified the extreme dry (wet) years as the scPDSI values below (above) a standard deviation of two. Spatial correlations between the reconstructed time series and SSTs were applied to investigate the influence of global SSTs on moisture variability in the study area, using the KNMI climate explorer (http://climexp.knmi.nl). The Extended Reconstructed SST Version 5 (ERSSTv5) was adopted for spatial correlations [37].

3. Results

3.1. Statistics of Tree Ring Chronology

The TRW chronology ranges from 1815 to 2014 CE, with a mean segment length of 117 years (Figure 4). The mean sensitivity (MS) of the TRW chronology is 0.29. The standard deviation (SD) and first-order autocorrelation (AC1) are 0.21 and 0.65, respectively (Table 1). According to the EPS cutoff value 0.85 [32], the reliable portion of the TRW chronology spans from 1894 to 2014. The Rbar ranges from 0.20 to 0.30, with an average value of 0.26. Based on these statistics, the TRW chronology is suitable for dendroclimatic reconstruction.

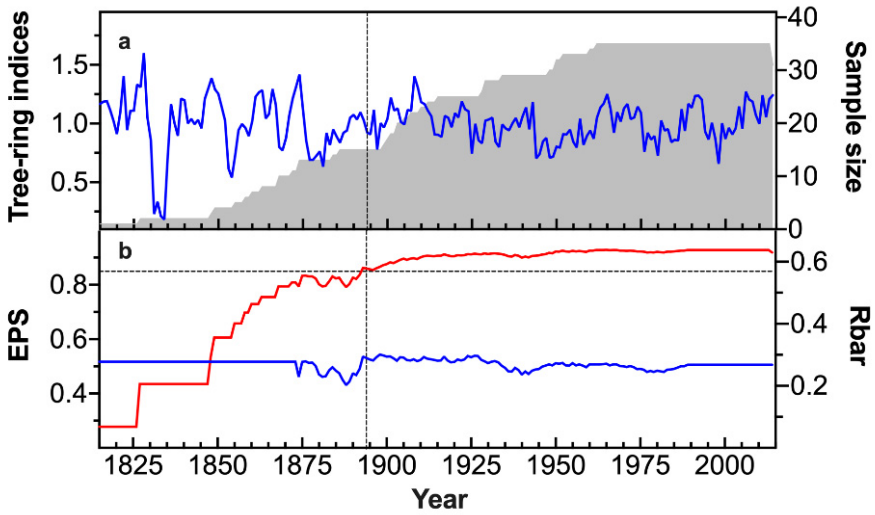

Figure 4. (**a**) TRW chronology at the XHS site in the east Pearl River basin, and the corresponding sample size (gray shading) and (**b**) the running EPS (red) and Rbar (blue) statistics calculated with a 51-year window. Horizontal dashed line in (**b**) denotes the 0.85 cutoff value. Vertical dashed line indicates the beginning of reliable period where the EPS value is above 0.85.

3.2. Climate-Growth Relationship

The correlation coefficients between the TRW chronology of *P. kwangtungensis* and monthly temperature and precipitation from Daoxian and Shaoguan meteorological stations are shown in Figure 5. Temperature from Daoxian station showed better correlations with tree growth than that from Shaoguan station, with significant positive correlations in the previous May, July, and August, and current September. The TRW chronology is significantly and negatively correlated with the previous July precipitation at Shaoguan, and the current October precipitation at Daoxian.

According to the above tree growth-climate relationship, *P. kwangtungensis* at the XHS site reflects the soil moisture balance condition. Therefore, correlations of the TRW chronology with the monthly scPDSI from nearby CRU grids were further carried out during their common period 1957–2014 during which the scPDSI data are mostly reliable (Figure 6). TRW chronology had significant negative correlations with the scPDSI from the previous March to the current October ($p < 0.05$). The correlations are more significant in months from the previous March to the current April, as well as the current August and September ($p < 0.01$). After comparing the highest correlation coefficients between TRW chronology and temperature, precipitation, and scPDSI, the pMay-cApr scPDSI was chosen to reflect the climatic signals encoded in tree rings.

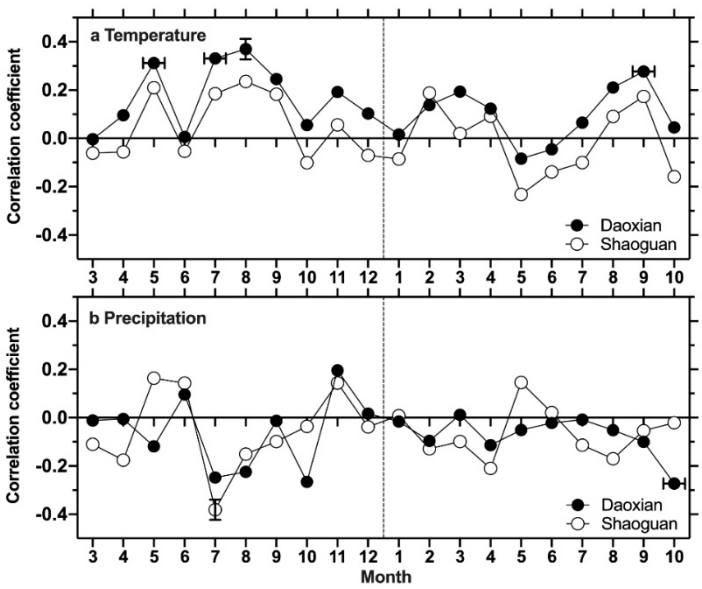

Figure 5. Correlation coefficients of the TRW chronology with (**a**) monthly mean temperature and (**b**) monthly total precipitation at Daoxian and Shaoguan meteorological stations from the previous March to the current October during their common period 1960–2014. Vertical dash lines separate previous and current year. Vertical mark denotes the 0.01 significance level. Horizontal mark denotes the 0.05 significance level.

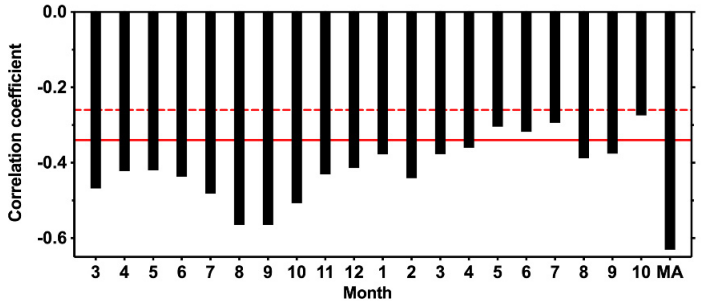

Figure 6. Correlations between TRW chronology and the monthly scPDSI records from the previous March to the current October during their common period 1957–2014. MA (previous May to current April) represents the target months for reconstruction. The solid (dash) line denotes the 0.01 (0.05) significance level, respectively.

3.3. scPDSI Reconstruction

Based on the climate-growth relationships at the XHS site, the pMay-cApr scPDSI was selected as the climatic variable for the reconstruction. The linear reconstruction model explains 39.9% (38.7% after adjustment for the loss of the degree of freedom) of the observed scPDSI variance during 1957–2014 (Figure 7a). The positive RE and CE statistics in the split period calibration/verification tests indicates good model skills (Table 2). A positive reduction of error (RE = 0.23) generated from the LOOCV test suggests that the reconstruction model is reliable. The first-differenced reconstructed and observed data were compared during their common period (Figure 7b). The correlation coefficient (r = 0.33, $p < 0.05$) and F value (F = 6.66, $p < 0.05$) are both statistically significant. These statistics together suggest that the robustness of the pMay-cApr scPDSI reconstruction.

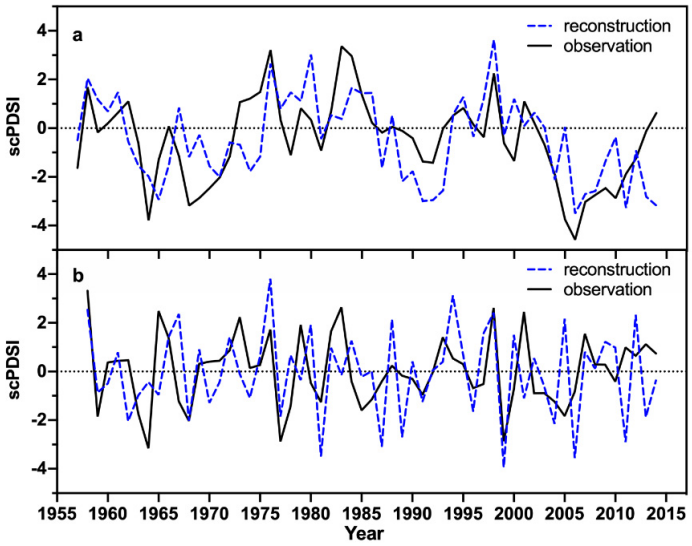

Figure 7. Comparisons of (**a**) observed (solid line) and reconstructed (dash line) pMay-cApr scPDSI during the common period 1957–2014, and (**b**) their first-differenced data during 1958–2014.

Table 2. Statistics of split calibration verification test results for the common period 1957–2014 CE.

Calibration				Verification		
Period	**R**	**R^2**	***p***	**Period**	**RE**	**CE**
1957–1985	0.522	0.27	0.002	1986–2014	0.353	0.164
1986–2014	0.495	0.25	0.003	1957–1985	0.327	0.187

R: Pearson correlation coefficient; R^2: coefficient of determination; *p*: *P*-value of statistical significance test; RE: reduction of error; CE: coefficient of efficiency.

Based on the regression model, the pMay-cApr scPDSI was reconstructed during the reliable period 1894–2014 (Figure 8). The mean and SD of the reconstructed scPDSI are −0.19 and 1.76, respectively. The top 10 driest and wettest years are listed in Table 3. The extremely dry/wet years are defined as the years with the scPDSI values lower/higher than 2 SD. There were two extremely dry years (1908 and 1909) and one extremely wet year (1998) over the reconstruction period. Decadal and multi-decadal variations were detected in the pMay-cApr scPDSI reconstruction. Based on an 11-year low-pass filter and its mean value, four dry periods (1899–1924, 1962–1974, 1988–1994, and 2003–2014) and four wet periods (1894–1898, 1925–1961, 1975–1987, and 1995–2002) were found in the reconstruction period from 1894 to 2014.

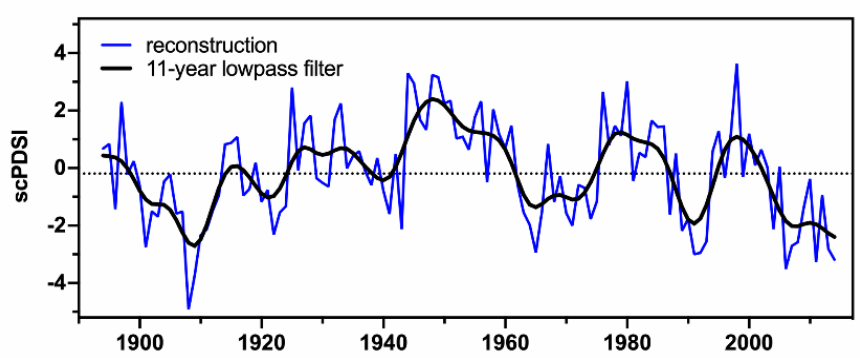

Figure 8. Tree ring-based scPDSI reconstruction (thin line) in the east Pearl River basin during the reliable period 1894–2014. The bold line denotes the series smoothed with 11-year low-pass filter. The horizontal dotted line denotes the mean value of the scPDSI reconstruction.

Table 3. The top 10 driest and wettest years of the pMay-cApr scPDSI reconstruction during 1894–2014 CE.

Rank	Dry Year	scPDSI	Wet Year	scPDSI
1	1908	−4.915	1998	3.631
2	1909	−3.740	1944	3.301
3	2006	−3.508	1948	3.236
4	2011	−3.271	1949	3.162
5	2014	−3.181	1980	3.023
6	1991	−2.995	1945	2.941
7	1992	−2.952	1925	2.806
8	1965	−2.936	1976	2.650
9	2013	−2.811	1951	2.340
10	1901	−2.754	1956	2.323

4. Discussion

4.1. The Climate-Tree Growth Relationship

The climate-tree growth relationships of *P. kwangtungensis* indicate that tree growth at the XHS site is sensitive to temperature and precipitation of the growing season in the previous year, especially the previous summer (Figure 5). Precipitation of the previous July was negatively correlated with *P. kwangtungensis* growth, while high temperature during the previous growing season benefits tree growth at the XHS site. This finding is supported by previous research showing that tree growth is not only influenced by climate conditions of the current year, but also that of the previous year [4,24]. For example, earlywood growth relies on current season photosynthates and carry-over carbohydrates from the previous year [38]. The TRW chronology at the XHS site had significant negative correlations with the scPDSI from the previous May to the current April, suggesting that tree growth is limited by moisture conditions in the east Pearl River basin. Many studies have shown the influence of moisture on tree growth in China, especially in semi-arid and semi-humid regions [21–23,39–44]. Unlike many other studies that showed a positive influence of moisture on tree growth as high moisture benefits cell division, cell enlargement and xylem formation during growing season [45–47], our results indicated that moisture had a negative impact on tree growth at XHS site, suggesting that relatively dry environment may favor radial growth. These negative correlations are possibly attributed to tree site conditions and tree species. *P. kwangtungensis* at XHS site grows on mountain slopes with thick soil and high water-holding capacity. As a result, trees may suffocate from lack of oxygen and/or die from root rot when the soil is waterlogged. The positive correlation between tree growth of *P. kwangtungensis* and growing season temperature may be related to reduced solar radiation under rainy periods, controlled by cloudiness frequency and duration, limiting photosynthetic rate, carbon uptake, and tree growth [48,49]. In the subtropical China, precipitation is abundant for *P. kwangtungensis* growth at the sampling site. However, excessive precipitation may dampen root water uptake by reducing soil transpiration rates and root hydraulic conductivity, which further decreases tree growth [50,51]. Overall, our study shows that water balance in the soil is crucial for *P. kwangtungensis* growth in South China. Under the background of global warming, the future drying environment in the Pearl River basin may be favorable for tree growth of *P. kwangtungensis*.

4.2. Tree Ring-Based scPDSI Variability and Spatial Representativeness

Decadal and multi-decadal variations can be detected in the pMay-cApr scPDSI reconstruction. Four drought periods (1899–1924, 1962–1974, 1988–1994, and 2003–2014) and four wet periods (1894–1898, 1925–1961, 1975–1987, and 1995–2002) are found in the reconstruction over 1894–2014. To validate the major drought and wet periods in the scPDSI reconstruction, three PDSI and/or precipitation reconstructions in Southeast China were selected for comparison [52–54]. The major drought between the 1900s and the 1920s in this study agrees well with the tree ring δ^{18}O-based

June–October PDSI reconstruction in Mt. Tianmu, Southeast China [52]. The major wet period in the 1940s–1950s in this study is consistent with the monsoon Asian precipitation index reconstructed by merging tree rings and historical documentary records, and with a tree ring δ^{18}O-based May–October precipitation reconstruction in Southeast China [53,54]. The spatial representativeness of our scPDSI reconstruction is reflected in the spatial correlation with the CRU gridded scPDSI over their common period 1957–2014 (Figure 9). The regions with the highest correlations were found at the southeast of the tree ring site, which were consistent with the highest correlations between the TRW chronology and the CRU gridded scPDSI data that were selected for reconstruction (Figure 1). Large-scale significant correlations indicate that the TRW chronology at the XHS site can effectively represent the regional scPDSI variability in the Pearl River basin.

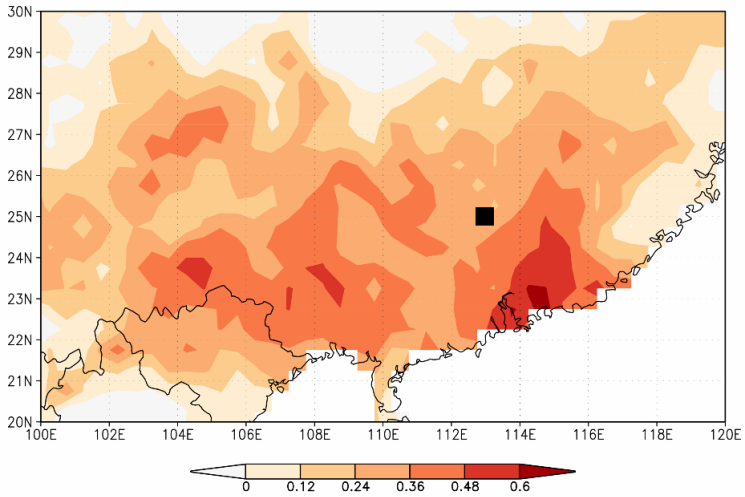

Figure 9. Spatial correlations between the reconstructed scPDSI and the CRU gridded scPDSI during 1957–2014. The black square denotes the tree ring sample site in this study.

4.3. Linkages of the scPDSI Variability to Pacific SSTs

To explore the linkages of the moisture variability in the study area to the Pacific and Indian Ocean SSTs, a spatial correlation analysis between the reconstructed scPDSI and global SSTs was analyzed during 1957–2014 (Figure 10). The spatial correlation pattern shows that the reconstructed scPDSI is significantly and negatively correlated with northern and western Pacific SSTs and positively correlated with eastern Pacific SSTs, suggesting that SST variability in these domains has a strong influence on moisture availability in the study area. The climate in the Pearl River basin is dominated by the East Asian monsoon with moisture supply from the western Pacific and Indian Ocean [55,56]. An intensified western Pacific high and Asian summer monsoon could lead to more precipitation in south China [57,58]. Previous studies suggested that the Pacific Decadal Oscillation (PDO) and the El Niño/Southern Oscillation (ENSO) influence the precipitation variability in the Pearl River basin, and the strengthening anticyclonic circulation could affect extreme precipitation changes via increasing geopotential height and weakening monsoonal flow [59]. Many studies have also pointed out that the PDO may influence tree growth or PDSI variability in Southeast China through its influence on the East Asian summer monsoon [24,52,60]. The spatial correlation of our scPDSI reconstruction with the global SSTs also manifests a weak PDO pattern (Figure 10), which is consistent with previous studies.

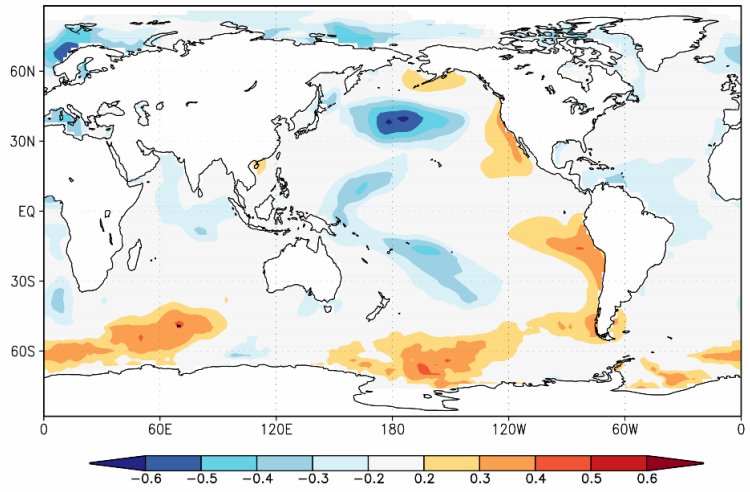

Figure 10. Spatial correlations of the reconstructed pMay-cApr scPDSI with global SST during 1957–2014.

5. Conclusions

A TRW chronology of *P. kwangtungensis* ranging from 1815 to 2014 was developed in the east Pearl River basin, which enables a pMay-cApr scPDSI reconstruction based on the climate-tree growth relationship. Spatial correlation analysis with the CRU gridded scPDSI data indicates that the reconstruction can effectively represent the large-scale scPDSI variability in the region. Decadal and multi-decadal variations in the study area were detected in the scPDSI reconstruction during 1894–2014. Significant correlations with the Pacific SSTs suggest that the latter exerts strong influence on moisture variability in the Pearl River basin. Future research should be devoted to the development of a larger tree ring network with longer chronologies in the Pearl River basin and the exploration of the mechanisms of climate impact on tree growth in subtropical regions.

Author Contributions: Conceptualization, T.L. and J.L.; methodology, T.L.; validation, T.L. and J.L.; formal analysis, T.L.; investigation, T.L., J.L. and T.F.A.; resources, J.L.; data curation, T.L.; writing—original draft preparation, T.L.; writing—review and editing, J.L., T.F.A. and D.D.Z.; visualization, T.L.; supervision, J.L. and D.D.Z.; project administration, J.L.; funding acquisition, J.L. and D.D.Z. All authors have read and agreed to the published version of the manuscript.

Funding: This research was funded by the National Key Research and Development Program of China (No. 2018YFA0605601), Hong Kong Research Grants Council (No. 17303017), and Key Platform Construction Project-Special Project of High-Level University Construction at Guangzhou University (No. 290020363).

Acknowledgments: We would like to thank Shengda Zhang from Guangzhou University for his kind assistance with GIS mapping. We are also grateful for the help of early field investigation and sampling of Waisum Ma from University of Birmingham.

Conflicts of Interest: The authors declare no conflict of interest.

References

1. Tian, Q.; Yang, S. Regional climatic response to global warming: Trends in temperature and precipitation in the Yellow, Yangtze and Pearl River basins since the 1950s. *Quat. Int.* **2017**, *440*, 1–11. [CrossRef]
2. Zhang, Q.; Xu, C.-Y.; Zhang, Z. Observed changes of drought/wetness episodes in the Pearl River basin, China, using the standardized precipitation index and aridity index. *Theor. Appl. Climatol.* **2009**, *98*, 89–99. [CrossRef]
3. Zhang, Q.; Li, J.; Gu, X.; Shi, P. Is the Pearl River basin, China, drying or wetting? Seasonal variations, causes and implications. *Glob. Planet. Chang.* **2018**, *166*, 48–61. [CrossRef]
4. Fritts, H.C. *Tree Rings and Climate*; Academic Press: London, UK, 1976.
5. Briffa, K.R.; Osborn, T.J.; Schweingruber, F.H.; Harris, I.C.; Jones, P.D.; Shiyatov, S.G.; Vaganov, E.A. Low-frequency temperature variations from a northern tree ring density network. *J. Geophys. Res. Atmos.* **2001**, *106*, 2929–2941. [CrossRef]

6. Cook, E.R.; Meko, D.M.; Stahle, D.W.; Cleaveland, M.K. Drought reconstructions for the continental United States. *J. Clim.* **1999**, *12*, 1145–1162. [CrossRef]
7. Büntgen, U.; Tegel, W.; Nicolussi, K.; McCormick, M.; Frank, D.; Trouet, V.; Kaplan, J.O.; Herzig, F.; Heussner, K.-U.; Wanner, H. 2500 years of European climate variability and human susceptibility. *Science* **2011**, *331*, 578–582.
8. Lara, A.; Villalba, R. A 3620-year temperature record from *Fitzroya cupressoides* tree rings in southern South America. *Science* **1993**, *260*, 1104–1106. [CrossRef]
9. Cook, E.; Bird, T.; Peterson, M.; Barbetti, M.; Buckley, B.; D'Arrigo, R.; Francey, R.; Tans, P. Climatic change in Tasmania inferred from a 1089-year tree-ring chronology of Huon Pine. *Science* **1991**, *253*, 1266–1268. [CrossRef]
10. Esper, J.; Cook, E.R.; Schweingruber, F.H. Low-frequency signals in long tree-ring chronologies for reconstructing past temperature variability. *Science* **2002**, *295*, 2250–2253. [CrossRef]
11. Till, C.; Guiot, J. Reconstruction of precipitation in Morocco since 1100 AD based on Cedrus atlantica tree-ring widths. *Quat. Res.* **1990**, *33*, 337–351. [CrossRef]
12. D'Arrigo, R.; Jacoby, G.; Frank, D.; Pederson, N.; Cook, E.; Buckley, B.; Nachin, B.; Mijiddorj, R.; Dugarjav, C.J.G.R.L. 1738 years of Mongolian temperature variability inferred from a tree-ring width chronology of Siberian pine. *Geophys. Res. Lett.* **2001**, *28*, 543–546. [CrossRef]
13. Shao, X.; Xu, Y.; Yin, Z.-Y.; Liang, E.; Zhu, H.; Wang, S. Climatic implications of a 3585-year tree-ring width chronology from the northeastern Qinghai-Tibetan Plateau. *Quat. Sci. Rev.* **2010**, *29*, 2111–2122. [CrossRef]
14. Zhang, Q.B.; Cheng, G.; Yao, T.; Kang, X.; Huang, J. A 2,326-year tree-ring record of climate variability on the northeastern Qinghai-Tibetan Plateau. *Geophys. Res. Lett.* **2003**, *30*. [CrossRef]
15. Yang, B.; Qin, C.; Wang, J.; He, M.; Melvin, T.M.; Osborn, T.J.; Briffa, K.R. A 3,500-year tree-ring record of annual precipitation on the northeastern Tibetan Plateau. *Proc. Natl. Acad. Sci. USA* **2014**, *111*, 2903–2908. [CrossRef] [PubMed]
16. Li, J.; Xie, S.-P.; Cook, E.R.; Huang, G.; D'arrigo, R.; Liu, F.; Ma, J.; Zheng, X.-T. Interdecadal modulation of El Niño amplitude during the past millennium. *Nat. Clim. Chang.* **2011**, *1*, 114–118. [CrossRef]
17. Bi, Y.; Xu, J.; Gebrekirstos, A.; Guo, L.; Zhao, M.; Liang, E.; Yang, X. Assessing drought variability since 1650 AD from tree-rings on the Jade Dragon Snow Mountain, southwest China. *Int. J. Climatol.* **2015**, *35*, 4057–4065. [CrossRef]
18. Chen, F.; Yuan, Y.; Wei, W.; Yu, S.; Wang, H. tree-ring response of subtropical tree species in southeast China on regional climate and sea-surface temperature variations. *Trees* **2015**, *29*, 17–24. [CrossRef]
19. Cai, Q.; Liu, Y.; Liu, H.; Sun, C.; Wang, Y. Growing-season precipitation since 1872 in the coastal area of subtropical southeast China reconstructed from tree rings and its relationship with the East Asian summer monsoon system. *Ecol. Indic.* **2017**, *82*, 441–450. [CrossRef]
20. Fang, K.; Cai, B.; Liu, X.; Lei, G.; Jiang, X.; Zhao, Y.; Li, H.; Seppä, H. Climate of the late Pleistocene and early Holocene in coastal South China inferred from submerged wood samples. *Quat. Int.* **2017**, *447*, 111–117. [CrossRef]
21. Li, D.; Fang, K.; Li, Y.; Chen, D.; Liu, X.; Dong, Z.; Zhou, F.; Guo, G.; Shi, F.; Xu, C. Climate, intrinsic water-use efficiency and tree growth over the past 150 years in humid subtropical China. *PLoS ONE* **2017**, *12*, e0172045. [CrossRef]
22. Chen, F.; Yuan, Y.; Wei, W.; Yu, S.; Zhang, T. Tree ring-based winter temperature reconstruction for Changting, Fujian, subtropical region of Southeast China, since 1850: Linkages to the Pacific Ocean. *Theor. Appl. Climatol.* **2012**, *109*, 141–151. [CrossRef]
23. Chen, F.; Yuan, Y.-J.; Wei, W.-S.; Yu, S.-L.; Zhang, T.-W. Reconstructed temperature for Yong'an, Fujian, Southeast China: Linkages to the Pacific Ocean climate variability. *Glob. Planet. Chang.* **2012**, *86*, 11–19. [CrossRef]
24. Dong, Z.; Chen, D.; Du, J.; Yang, G.; Bai, M.; Zhou, F.; Zheng, Z.; Ruan, C.; Fang, K. A 241-Year Cryptomeria fortune tree-ring Chronology in Humid Subtropical China and Its Linkages with the Pacific Decadal Oscillation. *Atmosphere* **2020**, *11*, 247. [CrossRef]
25. Wu, Z.; Raven, P.H. *Flora of China*; Science Press: Beijing, China; Missouri Botanical Garden: St. Louis, MO, USA, 1999; Volume 4.
26. Holmes, R.L. Computer-assisted quality control in tree-ring dating and measurement. *Tree-Ring Bull.* **1983**, *43*, 69–78.

27. Cook, E.R.; Kairiukstis, L.A. *Methods of Dendrochronology: Applications in the Environmental Sciences*; Springer Science & Business Media: Berlin/Heidelberg, Germany, 1990.
28. Melvin, T.M.; Briffa, K.R.; Nicolussi, K.; Grabner, M. Time-varying-response smoothing. *Dendrochronologia* **2007**, *25*, 65–69. [CrossRef]
29. Frank, D.; Esper, J.; Cook, E.R. Adjustment for proxy number and coherence in a large-scale temperature reconstruction. *Geophys. Res. Lett.* **2007**, *34*, L16709. [CrossRef]
30. Osborn, T.; Briffa, K.; Jones, P. Adjusting variance for sample size in tree-ring chronologies and other regional mean timeseries. *Dendrochronologia* **1997**, *15*, 89–99.
31. Melvin, T.M.; Briffa, K.R. A "signal-free" approach to dendroclimatic standardisation. *Dendrochronologia* **2008**, *26*, 71–86. [CrossRef]
32. Wigley, T.M.; Briffa, K.R.; Jones, P.D. On the average value of correlated time series, with applications in dendroclimatology and hydrometeorology. *J. Clim. Appl. Meteor.* **1984**, *23*, 201–213. [CrossRef]
33. Palmer, W.C. *Meteorological Drought*; US Department of Commerce, Weather Bureau: Silver Spring, MD, USA, 1965; Volume 30.
34. Wells, N.; Goddard, S.; Hayes, M.J. A self-calibrating Palmer drought severity index. *J. Clim.* **2004**, *17*, 2335–2351. [CrossRef]
35. Harris, I.C.; Jones, P.D. *CRU TS4.01: Climatic Research Unit (CRU) Time-Series (TS) Version 4.01 of High-Resolution Gridded Data of Month-by-Month Variation in Climate (Jan. 1901–Dec. 2016)*, 4 December 2017 ed.; Centre for Environmental Data Analysis: Leeds, UK; University of East Anglia Climatic Research Unit: Norwich, UK, 2017. [CrossRef]
36. Michaelsen, J. Cross-validation in statistical climate forecast models. *J. Clim. Appl. Meteor.* **1987**, *26*, 1589–1600. [CrossRef]
37. Huang, B.; Thorne, P.W.; Banzon, V.F.; Boyer, T.; Chepurin, G.; Lawrimore, J.H.; Menne, M.J.; Smith, T.M.; Vose, R.S.; Zhang, H.-M. Extended reconstructed sea surface temperature, version 5 (ERSSTv5): Upgrades, validations, and intercomparisons. *J. Clim.* **2017**, *30*, 8179–8205. [CrossRef]
38. Kagawa, A.; Sugimoto, A.; Maximov, T.C. $^{13}CO_2$ pulse-labelling of photoassimilates reveals carbon allocation within and between tree rings. *Plant Cell Environ.* **2006**, *29*, 1571–1584. [CrossRef] [PubMed]
39. Fan, Z.; Bräuning, A.; Cao, K. tree-ring based drought reconstruction in the central Hengduan Mountains region (China) since AD 1655. *Int. J. Climatol.* **2008**, *28*, 1879–1887. [CrossRef]
40. Fang, K.; Gou, X.; Chen, F.; Li, J.; D'Arrigo, R.; Cook, E.; Yang, T.; Davi, N. Reconstructed droughts for the southeastern Tibetan Plateau over the past 568 years and its linkages to the Pacific and Atlantic Ocean climate variability. *Clim. Dyn.* **2010**, *35*, 577–585. [CrossRef]
41. Fang, K.; Gou, X.; Chen, F.; Yang, M.; Li, J.; He, M.; Zhang, Y.; Tian, Q.; Peng, J. Drought variations in the eastern part of northwest China over the past two centuries: Evidence from tree rings. *Clim. Res.* **2009**, *38*, 129–135. [CrossRef]
42. Li, J.; Shi, J.; Zhang, D.D.; Yang, B.; Fang, K.; Yue, P.H. Moisture increase in response to high-altitude warming evidenced by tree-rings on the southeastern Tibetan Plateau. *Clim. Dyn.* **2017**, *48*, 649–660. [CrossRef]
43. Peng, J.; Liu, Y. Reconstructed droughts for the northeastern Tibetan Plateau since AD 1411 and its linkages to the Pacific, Indian and Atlantic Oceans. *Quat. Int.* **2013**, *283*, 98–106. [CrossRef]
44. Wang, X.; Zhang, Q.; Ma, K.; Xiao, S. A tree-ring record of 500-year dry-wet changes in northern Tibet, China. *Holocene* **2008**, *18*, 579–588. [CrossRef]
45. Hsiao, T.C.; Acevedo, E. Plant responses to water deficits, water-use efficiency, and drought resistance. In *Developments in Agricultural and Managed Forest Ecology*; Elsevier: Amsterdam, The Netherlands, 1975; Volume 1, pp. 59–84.
46. Au, T.F.; Maxwell, J.T.; Novick, K.A.; Robeson, S.M.; Warner, S.M.; Lockwood, B.R.; Phillips, R.P.; Harley, G.L.; Telewski, F.W.; Therrell, M.D.; et al. Demographic shifts in eastern US forests increase the impact of late-season drought on forest growth. *Ecography* **2020**, *43*, 1475–1486. [CrossRef]
47. Martin-Benito, D.; Pederson, N. Convergence in drought stress, but a divergence of climatic drivers across a latitudinal gradient in a temperate broadleaf forest. *J. Biogeogr.* **2015**, *42*, 925–937. [CrossRef]
48. Rozas, V.; Zas, R.; García-González, I. Contrasting effects of water availability on *Pinus pinaster* radial growth near the transition between the Atlantic and Mediterranean biogeographical regions in NW Spain. *Eur. J. For. Res.* **2011**, *130*, 959–970. [CrossRef]

49. Graham, E.A.; Mulkey, S.S.; Kitajima, K.; Phillips, N.G.; Wright, S.J. Cloud cover limits net CO_2 uptake and growth of a rainforest tree during tropical rainy seasons. *Proc. Natl. Acad. Sci. USA* **2003**, *100*, 572–576. [CrossRef] [PubMed]
50. Caldwell, M.M.; Richards, J.H. Hydraulic lift: Water efflux from upper roots improves effectiveness of water uptake by deep roots. *Oecologia* **1989**, *79*, 1–5. [CrossRef]
51. Ritchie, J. Soil water balance and plant water stress. In *Understanding Options for Agricultural Production*; Springer: Berlin/Heidelberg, Germany, 1998; pp. 41–54.
52. Liu, Y.; Fang, C.X.; Li, Q.; Song, H.M.; Ta, W.Y.; Zhao, G.J.; Sun, C.F. tree-ring $\delta^{18}O$ based PDSI reconstruction in the Mt. Tianmu region since 1618 AD and its connection to the East Asian summer monsoon. *Ecol. Indic.* **2019**, *104*, 636–647. [CrossRef]
53. Shi, H.; Wang, B.; Cook, E.R.; Liu, J.; Liu, F. Asian Summer Precipitation over the Past 544 Years Reconstructed by Merging Tree Rings and Historical Documentary Records. *J. Clim.* **2018**, *31*, 7845–7861. [CrossRef]
54. Xu, C.X.; Ge, J.Y.; Nakatsuka, T.; Yi, L.; Zheng, H.Z.; Sano, M. Potential utility of tree ring $\delta^{18}O$ series for reconstructing precipitation records from the lower reaches of the Yangtze River, southeast China. *J. Geophys. Res. Atmos.* **2016**, *121*, 3954–3968. [CrossRef]
55. Wang, B.; Wu, R.; Fu, X. Pacific-East Asian teleconnection: How does ENSO affect East Asian climate? *J. Clim.* **2000**, *13*, 1517–1536. [CrossRef]
56. Böhner, J. General climatic controls and topoclimatic variations in Central and High Asia. *Boreas* **2006**, *35*, 279–295. [CrossRef]
57. Zhang, R.; Sumi, A.; Kimoto, M. A diagnostic study of the impact of El Nino on the precipitation in China. *Adv. Atmos. Sci.* **1999**, *16*, 229–241. [CrossRef]
58. Li, T.; Zhang, Y.; Chang, C.P.; Wang, B. On the relationship between Indian Ocean sea surface temperature and Asian summer monsoon. *Geophys. Res. Lett.* **2001**, *28*, 2843–2846. [CrossRef]
59. Zhao, Y.; Zou, X.; Cao, L.; Xu, X. Changes in precipitation extremes over the Pearl River Basin, southern China, during 1960–2012. *Quat. Int.* **2014**, *333*, 26–39. [CrossRef]
60. Li, Y.; Fang, K.; Cao, C.; Li, D.; Zhou, F.; Dong, Z.; Zhang, Y.; Gan, Z. A tree-ring chronology spanning 210 years in the coastal area of southeastern China, and its relationship with climate change. *Clim. Res.* **2016**, *67*, 209–220. [CrossRef]